# Non-Heme (Inorganic) Iron (II) is a Possible Primary Activator of Artemisinin in *Plasmodium falciparum*-Infected Erythrocytes

Nurhidanatasha Abu Bakar

*School of Health Sciences, Health Campus, Universiti Sains Malaysia, 16150 Kubang Kerian, Kelantan, Malaysia.*

Corresponding author: natashaa@usm.my

**ABSTRACT**: Artemisinin (ART) possesses a unique endoperoxide pharmacophore that undergoes a reductive cleavage by iron (Fe) species for its antimalarial action. The role of Fe in the catalytic activation of ART is however still a matter of debate. Isobologram analysis was used to examine the interaction of ART with the Fe(III) chelator, desferrioxamine (DFO). We found that DFO strongly antagonizes ART action against the parasite (SFIC >2.0). The chelation of Fe(III) might alter the equilibrium between Fe(III) and Fe(II) thus reducing the concentration of Fe(II)that is essential for ART activation. Similar antagonism was observed between the Fe(II) chelator, TPEN [N,N,N',N-tetrakis (2-pyridylmethyl) ethylenediamine] and ART. Spectrophotometric studies suggested that ferrous heme but not ferric heme can also activate ART; however TPEN and DFO bind weakly to ferrous heme and ferric heme, respectively. This indicates that non-hemeFe (II) is a possible primary activator of ART in the malaria parasite.

**Keywords**: *Plasmodium falciparum*, iron, heme, artemisinin, desferrioxamine, TPEN

## Introduction

Artemisinin (ART) is one of the key drugs used in artemisinin-based combination therapies in the fight against malaria. It shows potent antimalarial activity, very rapid action, and no toxicity in clinical applications (Miller *et al.*, 2013). It is widely accepted that the activity of ART derives from its endoperoxide bridge, a chemical feature that is found only in this class of antimalarials. Two main models of the cleavage of the endoperoxide bridge particularly by

redox active ferrous heme [ferroprotoporphyrin IX or FPFe(II)] (Meunier and Robert 2010) and ferrous iron [Fe(II)] (Haynes *et al.,* 2007) have been proposed for its antimalarial action. Both of which have led to the formation of highly electrophilic free radicals, which are thought to react with specific malaria parasite biomolecules (Li *et al.*,2005; Eckstein-Ludwig *et al.*,2003; Bhisuttibhan and Meshnick 2001). In infected erythrocytes, parasites ingest and transport hemoglobin-rich erythrocyte cytoplasm in vesicles to the digestive vacuole (DV) for separation of heme and globin (Abu Bakar *et al.,* 2010). Because large quantities of Fe accumulate in the DV, free Fe and heme thus have been studied as the key molecules participating in ART activation processes (Woodrow *et al.,* 2005).

Ferric heme[ferriprotoporphyrin IX or FPFe(III)] has been reported to react with ART by spectroscopic (Bilia *et al.,* 2002) and ESI-MS/HPLC (Messori *et al.,* 2003) analysis. The reaction between FPFe(III) with ART was, however, very slow (not reaching completion in 24 hours at 37°C) (Meshnick, 2003). Other authors have reported that ferrous heme[ferroprotoporphyrin IX or FPFe(II)] activates ART through *in situ* reduction of FPFe(III) by glutathione within 1 hour at 37°C (Robert *et al.,* 2002). Other *in vivo* and *in vitro* studies support the role for non-heme (inorganic) Fe in ART activation process. For example, the Fe(III) chelator, desferrioxamine (DFO) was used in an effort to examine the mechanism of action of ART (Ferrer *et al.*,2012; Stocks *et al.*,2007; Eckstein-Ludwig *et al.*,2003) although this chelator may be effective against both free Fe and heme. This has led to the suggestion that the interaction of free Fe(II) with ART represents a competitive pathway in catalyzing the cleavage of the endoperoxide bridge (Haynes *et al.,* 2007). Metal chelators that bind preferentially to Fe(II) might therefore be useful in an attempt to elucidate the importance of Fe(II) in ART activation. TPEN [N,N,N',N-tetrakis (2-pyridylmethyl) ethylenediamine] is selective for zinc(II) [Zn(II)] [the binding constant, $K_a$ of TPEN-Zn(II) binding = $10^{15.6}$ $M^{-1}$] but it also binds to Fe(II) with just one order of magnitude lower than that for Zn(II) [$K_a$ of TPEN-Fe(II) binding = $10^{14.6}$ $M^{-1}$] (Arslan *et al.*,1985).

In the present study, the interactions of DFO with FPFe(III) and TPEN with FPFe(II) were investigated in an effort to elucidate the molecular basis of antagonism of ART action. *In vitro* interactions were investigated using ultraviolet-visible (UV-Vis) spectrophotometric analysis and cellular interactions of ART with DFO and TPEN were examined using isobologram analysis of effects on parasite growth.

## Materials and methods

### *Isobologram analysis*

### *Parasite cultivation*

*P. falciparum* (D10 strain) was continuously cultured with type $O^+$erythrocytes suspended in complete culture medium containing RPMI 1640 (Gibco BRL, Invitrogen) supplemented with 5% human serum (Red Cross Blood Bank, Melbourne, Australia), 0.25% Albumax II (Gibco BRL, Invitrogen) and hypoxanthine (Sigma) using a method modified from that of Trager and Jensen (1976). Parasites were incubated at a temperature of 37˚C in a humidified atmosphere of 94% $N_2$, 5% $CO_2$ and 1% $O_2$.The levels of parasitemia in the cultures were kept at ≤10% with 5% hematocrit.

### *Parasite growth inhibition assay*

The inhibitory concentration of ART and the Fe chelators used in combination assays that kills 50% of the parasites ($IC_{50}$) was first determined using the parasite growth inhibition assay (Desjardin *et al.*, 1979). Each compound in ethanol (e.g. ART and DFO, Sigma) or dimethyl sulfoxide (e.g.TPEN, Sigma) was twofold serially diluted in hypoxanthine-free medium and mixed with a parasite suspension plated at 1% parasitemia (2% hematocrit) in 96-well plates (NUNC$^{TM}$, Thermo Fischer Scientific). The final solvent concentration was <1%. The plates were stacked in a sterile incubation chamber, gassed for 3minutes and incubated at 37°C. After 24-hour incubation, tritiated ($^3$H)-hypoxanthine-containing medium (Amersham) (at a final concentration of 0.2 μCi/well) was added into the plates that were incubated for additional 24 hours. The plates were harvested onto Wallac printed glass fiber filter mats with a 96-well cell harvester (Perkin-Elmer). Each dried filter mat was placed in a tube containing scintillation fluid. The amount of radioactivity of the $^3$H-hypoxanthine incorporated into the parasitized material trapped in the mats relative to the amount incorporated by the untreated controls was determined with a scintillation counter (Wallac 1410, Pharmacia). Data were transferred to Excel software (Microsoft Inc.) and the $IC_{50}$ of each compound was determined from the growth curve obtained in triplicate from three different experiments.

*Drug combination assay*

The cellular interactions of ART with the Fe chelators were examined *in vitro* using the isobologram method based on their $IC_{50}$ obtained from the parasite growth inhibition assays (Kalkanidis *et al.,* 2002). Drug dilutions were made to allow the $IC_{50}$ of the individual compounds to fall at about the fourth twofold serial dilution. The dilutions of each of the two compounds were prepared in fixed ratios (**Figure 1**). For example, solution 1 to 6 for ART-DFO in combination assays with the parasites were prepared at 1000:0, 60:5000, 30:10000, 15:20000, 7.5:40000 and 0:80000, respectively (concentration ratios of ART-DFO in nM, with the solution 1 and 6 being each compound alone). The drug dilutions were prepared and mixed with the parasite suspensions plated at 1% parasitemia (2% hematocrit) in 96-well plates. The six fixed-ratios of the compounds were tested in triplicate from three different experiments and processed as for the standard parasite growth inhibition assay. Two $IC_{50}$s for each of the four combination ratios were calculated separately. Then, fractional inhibitory concentrations (FICs) and sum FICs (SFICs) were calculated as follows: For example in ART-DFO combination assays, FIC of ART = $IC_{50}$ of ART in combination/$IC_{50}$ of ART alone. The same equation was applied to DFO. FICs were used to construct isobolograms. SFIC = FIC ART + FIC DFO. The nature of interaction of ART with the Fe chelators was classified on the basis of the mean SFIC as follows: synergism as mean SFIC <0.5, antagonism as mean SFIC >2.0 and additivity as mean SFIC = 0 (Bell, 2005). To validate the indifferent effect, the activity of ART and itself was assayed.

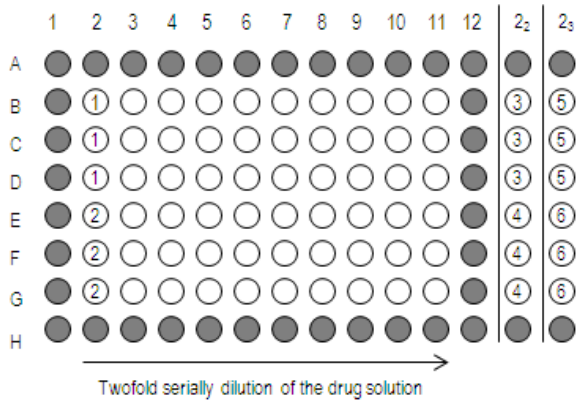


| Combination solution | Ratio of compound A & B | | Concentration ratios of ART-DFO [nM] | |
|---|---|---|---|---|
| | A | B | ART | DFO |
| 1 | 5 | 0 | 1000 | 0 |
| 2 | 4 | 1 | 60 | 5000 |
| 3 | 3 | 2 | 30 | 10000 |
| 4 | 2 | 3 | 15 | 20000 |
| 5 | 1 | 4 | 7.5 | 40000 |
| 6 | 0 | 5 | 0 | 100000 |

**Figure 1**: Outline of a combination assay on 96-well plates with the concentration ratios of compound A to B prepared as six solutions. When the plates were prepared as described in the text, wells labeled 1 to 6 served as drug wells for six drug combination solutions in triplicate with the wells in column 2 holding the highest drug concentration. Three 96-well plates were prepared similarly with column $2_2$ and $2_3$ representing solutions 3 to 4 and 5 to 6

in the second and third plates. Gray wells contained sterilized distilled water to avoid sample evaporation.

*Spectrophotometric analysis*

*Chemical reagents and instruments*

The reactions of ART with FPFe(III) and FPFe(II) were examined *in vitro* by spectrophotometric analysis (Taylor *et al.*, 2004). A stock solution of 1.5 mM FPFe(III) (Sigma-Aldrich) in 50 mM sodium hydroxide (NaOH) and stock solutions of 0.75, 1.5, 7.5, 15, 75 and 150 mM ART in ethanol were prepared. In order to generate FPFe(II) through reduction of FPFe(III), a small amount of sodium dithionite (DTN) was added in a working solution containing 50 mM sodium phosphate (pH 7.4, Sigma-Aldrich) and 0.5% sodium dodecyl sulfate (SDS, w/v in water, Sigma-Aldrich). All assays were carried out at 25°C and cuvette-based (Starna) with a 1.5 mL total volume of the working solution. Absorption spectra were monitored using a spectrophotometer (Cary 300) between 300-700 nm (a range of analytical wavelengths).

*Reaction of ART with FPFe(III) and FPFe(II)*

Various concentrations of ART (final concentrations of 5, 10, 50, 100, 500 and 1000 nM) from the respective stocks were added to the working solutions containing 10 µM FPFe(III) and 10 µM FPFe(II), respectively. Changes in the absorption band (the Soret band) of FPFe(III) and FPFe(II) in the absence and presence of ART were analyzed at 395 nm and 410 nm, respectively. The working solution with no FPFe(III) or FPFe(II) addition was used as a baseline control and subtracted from the spectra. The assays were performed in triplicate from three different occasions.

*Reaction of ART with FPFe(II) in the presence of the Fe chelators*

The assays were repeated in the presence of DFO and TPEN using an optimized concentration of ART that causes ~50% decrease of the Soret absorption band of FPFe(II). One mM DFO or TPEN (from their respective stock of 150 mM) was added to the working solution according to the protocols assigned in **Table 1**. Spectral changes of FPFe(III) in the presence of DFO

and FPFe(II) in the presence of TPEN were monitored and analyzed at 395 nm and 410 nm, respectively. The inhibitory effects (in percentage) of DFO and TPEN against reaction of ART with FPFe(II) were calculated as follows:

$$\text{Inhibitory effect (\%)} = (A + B) / B \times 100\%$$

A = Final absorption of FPFe(II) in the presence of the Fe chelator
B = Final absorption of FPFe(II) in the absence of the Fe chelator (control)

All values used in analysis are presented as means ± standard deviation (s.d.). Comparisons among the different groups were performed by one-way analysis of variance (ANOVA), followed by Bonferroni multiple comparisons test and the differences were considered significant when $P < 0.05$.

**Table 1**: Schematic protocols for reactions of ART with FPFe(II) in the presence of the Fe chelators, DFO and TPEN. Final concentrations of 10 µM of FPFe(III) and 50 µM of ART were used through all experiments. FPFe(II) was prepared from FPFe(III) by the addition of DTN. 1 mM DFO or TPEN was added in the order indicated in the table. Effects of DFO and TPEN were then examined spectrophotometrically by monitoring changes of the FPFe(II) absorption spectrum at 410 nm.

| GROUP | STEP 1 | STEP 2 | STEP 3 | STEP 4 |
|---|---|---|---|---|
| Negative control | **DFO / TPEN** | DTN | ART | - |
| Positive control | FPFe(III) | DTN reduces FPFe(III) =>FPFe(II) | ART | - |
| 1 | FPFe(III) + **DFO / TPEN** | DTN reduces FPFe(III) =>FPFe(II) | ART | - |
| 2 | FPFe(III) | DTN reduces FPFe(III) =>FPFe(II) | FPFe(II) +**DFO / TPEN** | ART |
| 3 | FPFe(III) | DTN FPFe(III) =>FPFe(II) | ART | FPFe(II) +**DFO / TPEN** |

*Binding of DFO to FPFe(III) and TPEN to FPFe(II)*

The binding constant for reactions of DFO with FPFe(III) and TPEN with FPFe(II) was determined using a titration assay. DFO and TPEN (from their respective stocks of 1.5, 7.5,

30 and 150 mM) were added to final concentrations ranging from 0.01-1 mM into FPFe(III)- and FPFe(II)-containing solutions, respectively. Solutions were mixed and 5 minutes were given for complete binding. Effects of DFO and TPEN on FPFe(III) and FPFe(II) spectra were monitored and analyzed at 395 nm and 410 nm, respectively. The binding constant of the reactions was determined from the curve of the ratio of the absorbance collected at two wavelengths [$A_{375/395}$ for DFO-FPFe(III) interaction; $A_{416}/_{410}$ for TPEN-FPFe(II) interaction] versus the iron chelator concentration. The assays were done in triplicate from three different occasions.

**Results and discussion**

*Reaction of ART with FPFe(III) and FPFe(II)*

ART absorbs weakly in the visible and near ultraviolet regions, precluding direct quantification or activation analysis. Therefore, changes in the characteristic Soret absorption band of FPFe(III) at 395 nm and FPFe(II) at 410 nm were used as a measure of their interactions with ART (Taylor *et al.*, 2004). The absorption spectra of FPFe(III) and FPFe(II) were compared without and with ART at various concentrations immediately after mixing in phosphate buffer solution. SDS (0.5%w/v in water) was used to maintain the hydrophobic nature of FPFe(III) or FPFe(II) and ART in buffer solution. The FPFe(III) or FPFe(II) concentration of 10 µM was selected and sufficient to provide adequate signal detection although much higher levels of their concentrations in the DV of the malaria parasite were reported (Sullivan *et al*., 1996).

The spectrophotometric profile of FPFe(III) (black dashed line) is shown in **Figure 2**. Even the highest concentration of ART (1 mM) produced no spectral change (**Figure 2**, pink line). Similar results were obtained by Zhang and Gerhard (2008) at pH 7.0 and 5.0 in phosphate buffer. We conclude that FPFe(III) does not bind directly to ART. FPFe(III) was then converted into FPFe(II) by the addition of DTN, causing the shift in the Soret band from 395 nm to 410 nm (**Figure 2**, red dashed line). DTN used as a reducing agent in this assay did not absorb at analytical wavelengths and its absorption spectrum did not change in the presence of ART (data not shown), excluding the possibility that ART was first activated by DTN (Zhang & Gerhard, 2008; Taylor *et al.*, 2004).). The addition of ART resulted in a decrease of the FPFe(II) Soret band in a concentration-dependent manner, presumably due to FPFe(II)-

induced activation of ART. The new absorption peak was observed at 462 nm following the reaction of ART with FPFe(II). This result indicates that FPFe(II) can activate ART, which in turn forms activated ART (Zhang & Gerhard 2008; Taylor *et al.*, 2004). Based on these spectrophotometric data, the concentration of ART that is associated with a 50% decrease of the Soret absorption band of FPFe(II) was ~50 µM. This ART concentration was used in the subsequent analysis of the effects of the Fe chelators on the activation of ART by FPFe(II).

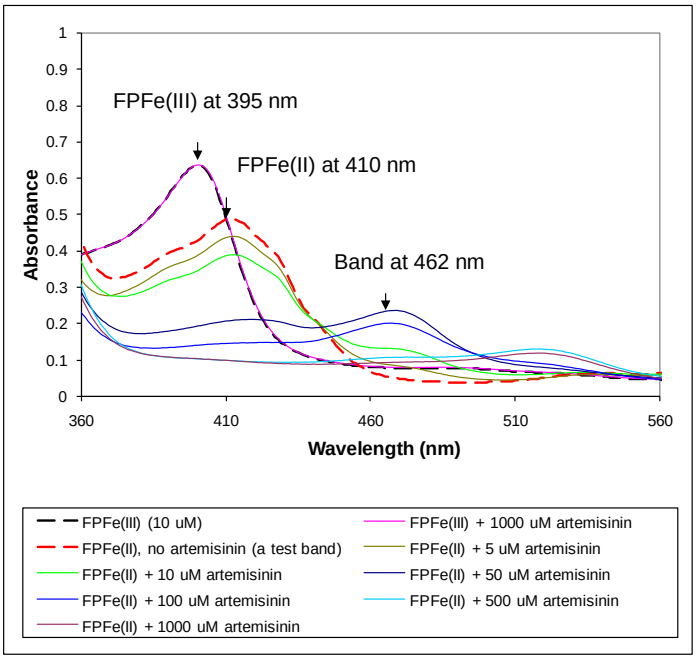


**Figure 2**: Activation of ART by FPFe(II) but not FPFe(III). Changes of the Soret absorption band of FPFe(III) and FPFe(II) (10 µM) were monitored at 395 nm and 410 nm, respectively, in the presence of ART (0.005-1 mM).The curves are from a single experiment and are representative of those obtained in three separate experiments.

*Effects of the Fe chelators on the reaction of ART with FPFe(II)*

Effects of DFO and TPEN on FPFe(II)-induced activation of ART were investigated *in vitro* according to the protocols described in **Table 1**. Changes in the Soret absorption band of FPFe(II) (10 µM) at 410 nm were used as a measure of the reaction of ART with FPFe(II) in the absence and presence of the Fe chelators. In the absence of DFO (positive control), the addition of ART (50 µM) led to a marked decrease of the FPFe(II) Soret band (69 ± 1%, **Figure 3A**). In the presence of DFO (1 mM) (Group 1), the decrease of the Soret band of FPFe(II) was significantly inhibited ($P < 0.05$) (49 ± 1%, **Figure 3A**). The results suggest that DFO can chelate FPFe(III) and in turn decrease the concentration of FPFe(II) available for

ART activation. The binding of DFO to FPFe(III) was shown by a hypsochromic shift (i.e. a change in the spectral position to a shorter wavelength) of the FPFe(III) absorption band from 395 nm (**Figure 3B**, red line) to 375 nm (blue line). However, the binding constant of DFO for FPFe(III) was modest ($K_a$ of DFO-FPFe(III) binding = 1 x $10^4$ $M^{-1}$, **Figure 3C**) confirming that DFO binds weakly to FPFe(III). No change in the FPFe(II) spectrum following the addition of DFO (Group 2) (**Figure 3D**, purple line) indicating that DFO does not bind directly to FPFe(II). When TPEN (1 mM) was added to FPFe(II) (Group 2) (**Figures 4B**, purple line), the Soret absorption band shifted from 410 nm to 416 nm (a bathochromic shift). This indicates that TPEN does indeed bind to FPFe(II) ($K_a$ of TPEN-FPFe(II) binding = 1 x $10^4$ $M^{-1}$, **Figures 4C**). However, no significant TPEN-mediated protection ($P > 0.05$) of the FPFe(II) Soret band was observed after the addition of ART (**Figure 4A** and **B**, brown line) although chelation of FPFe(II) by TPEN had clearly occurred. The results suggest that DFO and TPEN preferentially chelate free Fe(III) and Fe(II), respectively. They also bind weakly to FPFe(III) and FPFe(II) but do not appear to strongly antagonize FPFe(II)-mediated ART activation. It was reasoned that if Fe(II) is a major activator of ART *in vivo*, DFO and TPEN should antagonize Fe(II)-mediated ART activity against parasite cultures.

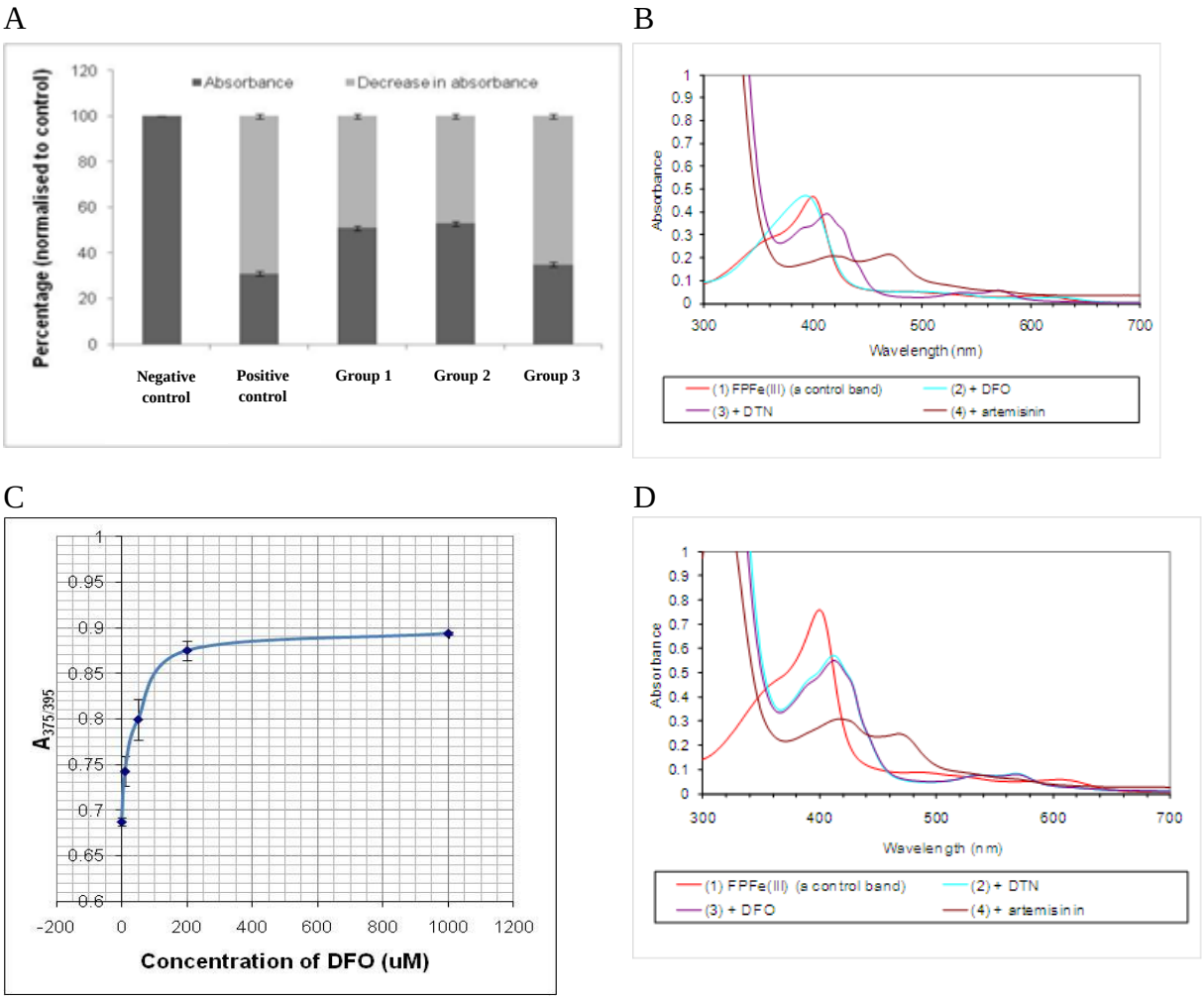


**Figure 3**: Effects of DFO on FPFe(II)-induced activation of ART. (A) The decrease (%) of the FPFe(II) Soret band (dark gray) and the inhibition (%) of the decrease of the FPFe(II) Soret band (light gray) in the absence and presence of DFO. The values were the mean ± s.d. from three separate experiments. (B) The shift of the FPFe(III) absorption band (red line) after DFO addition (blue line). C) Binding of DFO to FPFe(III). (D) No effect of DFO on the absorption spectrum of FPFe(II).

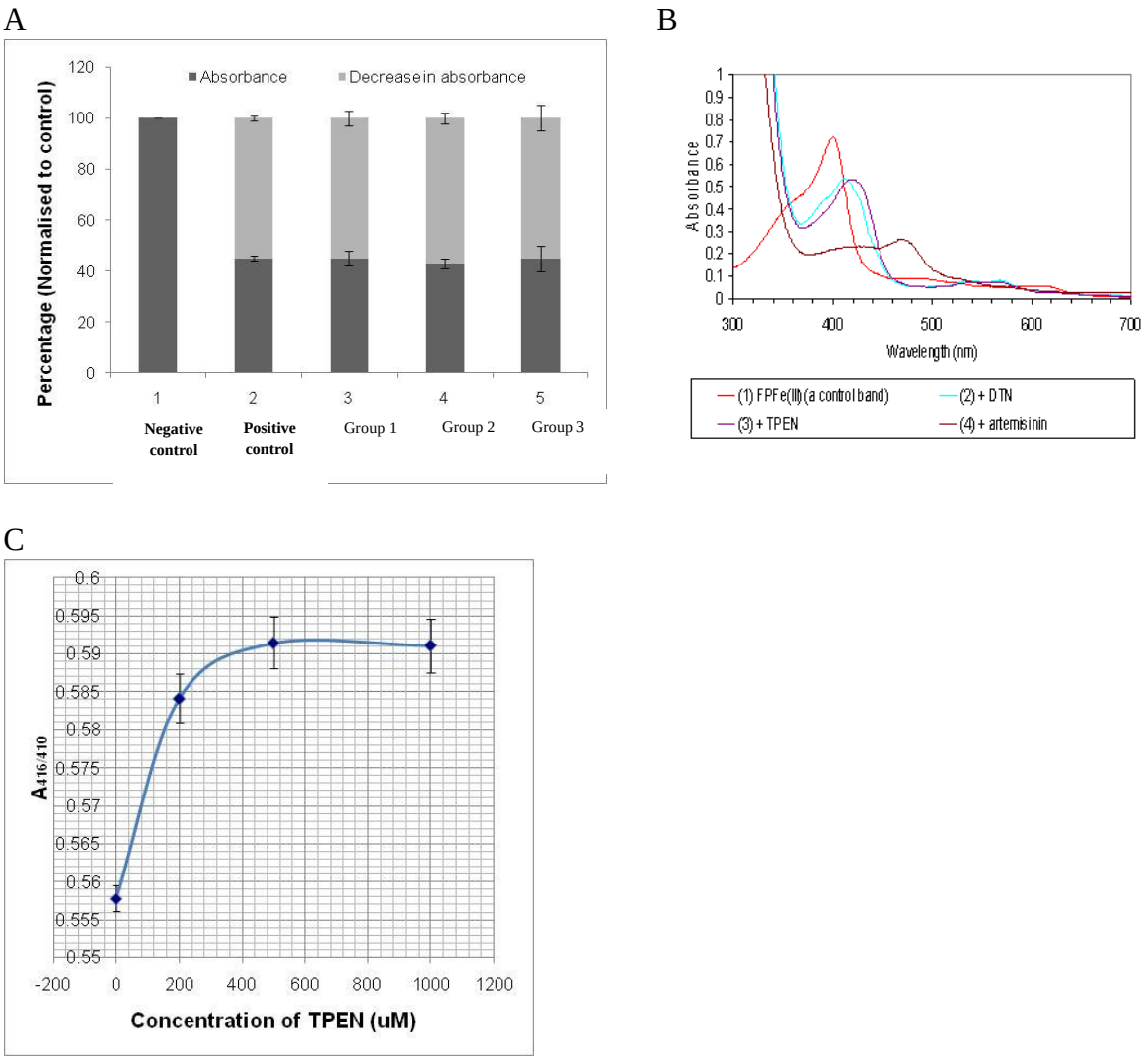


**Figure 4**: Effects of TPEN on FPFe(II)-induced activation of ART. (A) The decrease (%) of the FPFe(II) Soret band (dark gray) and the inhibition (%) of the decrease of the FPFe(II) Soret band (light gray) in the absence and presence of TPEN. The values were the mean ± s.d. from three separate experiments. (B) The shift of the FPFe(II) absorption band (blue line) after TPEN addition (purple line). C) Binding of TPEN to FPFe(III).

*Isobologram analysis of the interaction of ART with the Fe chelators*

Interactions of ART with the Fe chelators were investigated to provide clues as to their mechanisms of action (Kalkanidis *et al.*, 2002). Four different fixed-ratio combinations of ART and the Fe chelators were assigned based on their $IC_{50}$ values obtained previously from the parasite growth inhibition assays (**Figure 5**). The fractional inhibitory concentration (FIC) was calculated by dividing the apparent $IC_{50}$ value of ART in combination with the Fe chelators by the $IC_{50}$ value of ART when tested alone or vice versa. The FIC values in each

combination were added to give the sum of FICs (SFICs). These were used to generate the isobologram. A straight line, concave or convex curve indicates additivity, synergism or antagonism, respectively. The strength of interaction between the test compounds can be evaluated by the degree of deviation from the line of additivity (SFIC = 0). SFIC <0.5 is regarded as a strong synergism; strong antagonism is defined as a SFIC >2.0 (Bell 2005).

| Compound | Chemical structure | Mean $IC_{50}$ ± s.d. |
|---|---|---|
| Artemisinin | 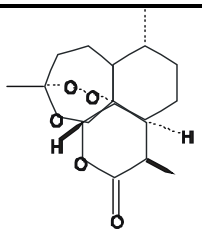 | 15 ± 4 nM |
| DFO | 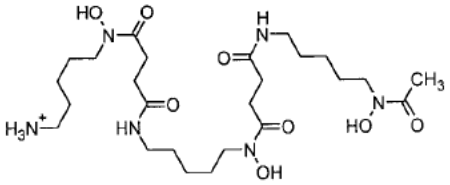 | 13 ± 3 µM |
| TPEN | 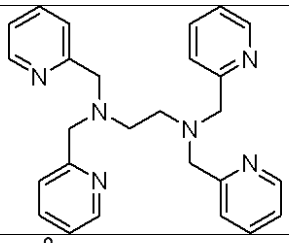 | 1.5 ± 1 µM |
| Zinquin | 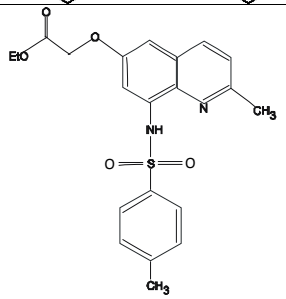 | 113 ± 18 µM |

**Figure 5**: Mean $IC_{50}$ values for inhibition of parasite growth by ART, and the iron chelators, DFO, TPEN and zinquin.

The isobologram of the interaction of ART with DFO demonstrated an antagonistic relationship (**Figure 5A**). This strong antagonism (SFIC >2.0) is similar to that reported previously (Stocks *et al.*, 2007). We propose that this is due to a strong chelation of free Fe(III) by DFO [$K_a$ of DFO-Fe(III) binding = $10^{31}$ $M^{-1}$] (Mabeza *et al.*, 1999) rather than by the weaker interaction of DFO with FPFe(III) [$K_a$ of DFO-FPFe(III) binding = $10^4$ $M^{-1}$]. The hexadentate binding units of DFO might fully occupy the coordination sites of free Fe(III),

thereby forming the most stable complex with this metal (Tam *et al.*, 2003). Besides Fe(III), DFO has an affinity for other tribasic metal cations such as aluminium(III) and gallium(III) (Mabeza *et al.*,1999; Lytton *et al.*, 1993). These metal cations however are available at only low concentrations in the parasite (Mabeza *et al.*, 1999). DFO also binds to Fe(II) [$K_a$ of DFO-Fe(II) binding = $10^{10}$ $M^{-1}$] (Mabeza *et al.*, 1999; Goodwin & Whitten 1965) and facilitates the oxidation of Fe(II) to Fe(III) (Harris & Aisen 1973). Binding of Fe(III) by DFO would in turn decrease the concentration of Fe(II) available for ART activation. This result is consistent with the suggestion that inorganic free Fe(II) is a possible major activator of ART.

Combinations of ART and TPEN (**Figure 5B**) or another Fe(II) chelator, zinquin (ZQ) (**Figure 5C**) also had an antagonistic effect. We propose that this is due to chelation of Fe(II) by ZQ or TPEN [$K_a$ of TPEN-Fe(II) binding = $10^{14.6}$ $M^{-1}$] (Arslan *et al.*, 1985), thereby reducing the amount of Fe(II) available for ART activation. It remains possible that the antagonistic effect of TPEN is due to chelation of Zn(II) [$K_a$ of TPEN-Zn(II) binding = $10^{15.6}$ $M^{-1}$] or manganese [Mn(II)] [$K_a$ of TPEN-Mn(II) binding = $10^{10.3}$ $M^{-1}$] (Arslan *et al.*, 1985). However Mn(II) is present at only low concentration in the parasite, while Zn(II) is a redox-inactive cation (Prasad, 2008; Dimitrova *et al.*, 2007). Thus, Fe(II) chelation appears the most likely reason for the antagonistic interaction of TPEN and ART.

Inhibition of FPFe(III) detoxification is thought to be central to the mechanism of action of the 4-aminoquinoline drug, chloroquine (CQ) (Foley & Tilley 1998; Dorn *et al.*, 1998). If CQ treatment leads to a buildup of heme in a form that can activate ART, it might be expected to be synergistic with ART. However, earlier studies reported an antagonistic effect between ART and CQ (Jaquet *et al.*, 1994; Chawira *et al.*, 1987). In this study, combinations of ART and CQ had an additive effect against the parasite (**Figure 5D**). The reason for the difference between this study and the previous study is still not clear. The lack of antagonism is however consistent with the suggestion that CQ binds to FPFe(III) and prevents its crystallization in the digestive vacuole while ART is activated by Fe(II) in the parasite cytoplasm.

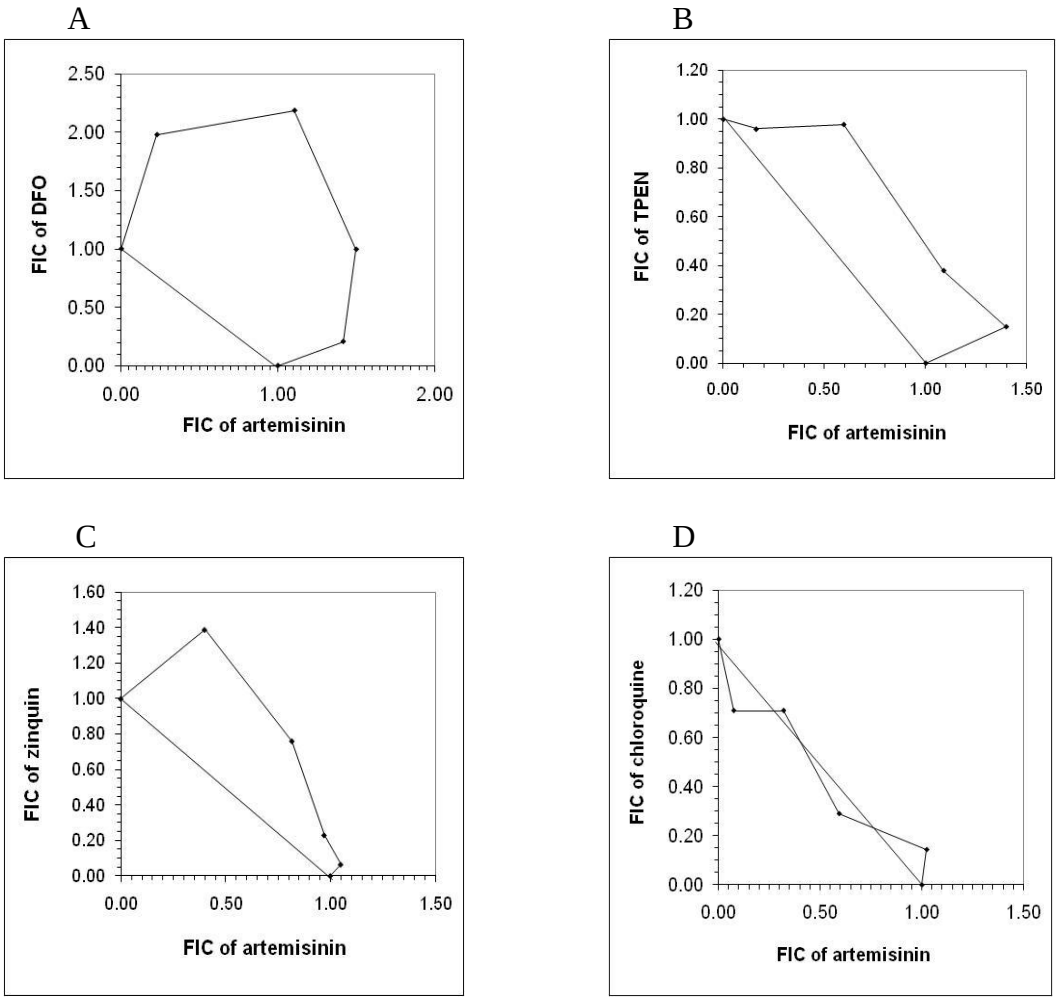


**Figure 6**: Isobologram analysis of the interactions of ART with the Fe chelators and quinoline antimalarial drug against *P. falciparum*-infected erythrocytes. Isobolograms were generated by plotting pairs of FICs for each combination of ART with the test compounds: (A) DFO, (B) TPEN, (C) ZQ and (D) chloroquine, CQ. Antagonistic effects were observed between ART and DFO, TPEN and ZQ (SFIC >1.0). Additive relationships were observed between ART and CQ (SFIC = 1.0).

## Conclusion

In the host erythrocyte, the malaria parasite is surrounded by hemoglobin, which is a ready source of nutrients and a potential source of Fe. The large amount of hemoglobin is degraded by the parasite for the bulk of amino acids, and the small amounts of Fe are released from heme during the detoxification process. The parasite requires Fe for the synthesis of Fe-containing proteins such as ribonucleotide reductase, superoxide dismutase and cytochrome. The high concentration of Fe within the malaria parasite also appears to be responsible for the ART action. Taken together the isobologram analysis and spectrophotometric data indicate that the antagonistic effects of DFO and TPEN are due to their strong chelation of Fe(III) and

Fe(II), respectively, thereby depleting the pool of free Fe(II) available for ART activation. Free Fe(II) activates and cleaves the endoperoxide bridge of ART, generating highly electrophilic free radicals. The findings suggest that free Fe(II) is a possible primary activator of ART in the malaria parasite-infected erythrocytes. Other potential sources of free Fe are serum Fe and erythrocyte Fe. However, these have never been certain; therefore further studies are needed to identify the source of parasite Fe, which is the target for a number of antimalarials including ART.

## Acknowledgement

The author thanks the Ministry of Higher Education, Malaysia and Universiti Sains Malaysia for the scholarship given from 2006-2010. I also gratefully acknowledge Dr. Nick Klonis and Prof. Dr. Leann Tilley, La Trobe University, Melbourne, Australia for the laboratory facilities and assistance during the experiments.

## References

Abu Bakar, N., Klonis, N., Hanssen, E., Chan, C. and Tilley, L. (2010). Digestive vacuole genesis and endocytic processes in the early intraerythrocytic stages of *Plasmodium falciparum. Journal Cell Sciences,* 123 (Pt 3):441-450.

Arslan, P., Di Virgilio, F. and Beltrame, M. (1985). Cytosolic $Ca^{2+}$ homeostasis in Ehrlich and Yoshida carcinoma. *Journal Biological Chemistry* 5(260): 2719-2727

Bell, A. (2005). Antimalarial drug synergism and antagonism: mechanistic and clinical significance. *FEMS Microbiology Letters.* 253: 171-184

Bhisutthibhan, J. and Meshnick, S. R. (2001).Immunoprecipitation of [3H]dihydroartemisinin translationally controlled tumor protein (TCTP) adducts from *Plasmodium falciparum*-infected erythrocytes by using anti-TCTP antibodies. *Antimicrobial Agents and Chemotherapy.* 45(8): 2397-2399

Bilia, A. R., Larazi, D., Messori, L., Taglioni, V., Temperini, C. and Vinciery, F. F. (2002). Simple and rapid physico-chemical methods to examine action of antimalarial drugs with hemin: its application to Artemisia annua constituents. *Life Sciences.* 70:769-778.

Chawira, A. N., Warhurst, D. C., Robinson, B. L. and Peters, W. (1987). The effect of combinations of qinghaosu (artemisinin) with standard antimalarial drugs in the

suppressive treatment of malaria in mice. *Transactions of the Royal Society of Tropical Medicine and Hygiene.* 81: 554-558

Desjardin, R. E., Canfield, C. J., Haynes, J. D. and Chulay, J. D. (1979). Quantitative assessment of antimalarial activity *in vitro* by a semiautomatedmicrodilution technique. *Antimicrobial Agents and Chemotherapy.* 16(6): 710-718

Dimitrova, A. A., Strashimirov, D. S., Russeva, A. L., Betova, T. M. and Tzachev, K. N. (2007). Changes in the activity of Cu/Zn superoxide dismutase, lipid profile and aorta morphology of spontaneously hypertensive rats on zinc. *Folia Medica.* 49(3-4): 52-57

Dorn, A., Vippagunta, S. R., Matile, H., Bubendorf, A. and Ridley, R. G. (1998).An assessment of drug-hematin binding as a mechanism for inhibition of hematin polymerization by quinolineantimalarials. *Biochemical Pharmacology.* 55: 727-736

Eckstein-Ludwig, U., Webb, R. J. I., van Goethem, D. A., East, J. M., Lee, A. G., Kimura, M., O‟ Neill, P.M., Bray, P. G., Ward, S. A. and Krishna, S. (2003). Artemisinins target the SERCA of *Plasmodium falciparum*. *Nature,* 424: 957-961

Ferrer, P., Tripathi, A. K., Clark, M. A., Hand, C. C., Rienhoff Jr., H. Y. and Sullivan, Jr. D. J (2012). Antimalarial iron chelator, FBS0701, shows asexual and gametocyte *Plasmodium falciparum* activity and single oral dose cure in a murine malaria model. *PloS ONE.* 7(5): e37171 (1-7).

Foley, M. and Tilley, L. (1998). Quinoline antimalarials: mechanisms of action and resistance and prospects for new agents. *Pharmacology & Therapeutics.* 79(1): 55-87

Goodwin, J. F. and Whitten, C. F. (1965).Chelation of ferrous sulphate solutions by desferrioxamine. *Nature,* 16(205): 281-283

Harris, D. C. and Aisen, P. (1973). Facilitation of Fe(II) autoxidation by Fe(III) complexing agents. *Biochimica et Biophysica Acta,* 329: 156-158

Haynes, R. K., Chan, W. C., Lung, C. M., Uhlemann, A. C., Eckstein, U., Taramelli, D., Parapini, S., Monti, D. and Krishna, S. (2007). The Fe(II)-mediated decomposition, *Pf*ATP6 binding, and antimalarial activities of artemisone and other artemisinins: the unlikelihood of C-centered radicals as bioactive intermediates. *ChemMedChem.* 2(10): 1480-1497

Jaquet, C., Stohler, H. R., Chollet, J. and Peters, W. (1994). Antimalarial activity of the bicyclic peroxide Ro 42-1611 (arteflene) in experimental models. *Tropical Medicine and Parasitology.* 45(3): 266-271

Kalkanidis, M., Klonis, N., Tilley, L. and Deady, L. W. (2002). Novel phenothiazine antimalarials: synthesis, antimalarial activity, and inhibition of the formation of β-haematin. *Biochemical Pharmacology.* 63(5): 833-842

Li, W., Mo, W., Shen, D., Sun, L., Wang, J., Lu, S., Gitschier, J. M. and Zhou, B. (2005). Yeast model uncovers dual roles of mitochondria in the action of artemisinin. *PLoS Genetics.* 1(3): e36

Lytton, S. D., Mester, B, Dayan, I., Glickstein, H., Shanzer, A. and Cabantchik, Z. I. (1993). Mode of action of iron(III) chelators as antimalarials. I. Membrane permeation properties and cytotoxic activity. *Blood.* 81: 214-221

Mabeza, G. F., Loyevsky, M., Gordeuk, V. R. and Weiss, G. (1999). Iron chelation therapy for malaria: a review. *Pharmacology & Therapeutics.* 81(1): 53-75

Meshnick, S. R. (2003). Artemisinin and heme. *Antimicrobial Agents and Chemotherapy.* 47(8): 2712, author reply 2712-2713.

Messori, L., Piccioli, F., Temperini, C., Bilia, A. R., Vincieri, F. F., Allegrozzi, M. and Turano, P. (2003). The reaction of artemisinin with hemin: a further insight into the mechanism. *Inorganica Chimica Acta.* 357:4602-4606.

Meunier, B. and Robert, A. (2010). Heme as trigger and target for trioxane-containing antimalarial drugs. *Accounts of Chemical Research.* 43: 1444-1451

Miller, L. H., Ackerman, H. C., Su, X. Z. and Wellems, T. E. (2013). Malaria biology and disease pathogenesis: insights for new treatments. *Nature Medicine.* 19: 156-167

Prasad, A. S. (2008). Zinc in human health: effect of zinc on immune cells. *Molecular Medicine.* 14(5-6): 353-357

Robert, A., Coppel, Y. and Meunier, B. (2002). Alkylation of heme by the antimalarial drug artemisinin. *Chemical Commununication (Cambridge, England).* 7(5):414-415.

Stocks, P. A., Bray, P. G., Bartob, V. E., Al-Helal, M., Jones, M., Araujo, N. C., Gibbons, P., Ward, S. A., Hughes, R. H., Biagini, G. A., Davies, J., Awemu, R., Mercer, A. E., Ellis, G. and O'Neil, P. M. (2007). Evidence for a common non-hemechetable-iron-dependent activation mechanis, for semisynthetic and synthetic endoperoxide antimalarial drugs. *Angewandte Chemie International Edition in English.* 119: 6394-6399

Sullivan, D. J., Gluzman, I. Y., Russell, D. G. and Goldberg, D. E. (1996). On the molecular mechanism of chloroquine's antimalarial action. *Proceedings of the National Academy of Sciences of the United State of America.* 93(21):11865-11870

Tam, T. F., Leung-Toung, R., Wanren, L., Wang, Y., Karimian, K. and Spino, M. (2003). Iron chelator research: past, present and future. *Current Medicinal Chemistry.* 10: 983-995

Taylor, D. K., Avery, T. D., Greatrex, B. W., Tiekink, E. R. T., Macreadie, I. G., Macreadie, P. I., Humphries, A. D., Kalkanidis, M., Fox, E. N., Klonis, N. and Tilley, L. (2004). Novel endoperoxide antimalarials: synthesis, heme-binding and antimalarial activity. *Journal of Medicinal Chemistry.* 47(7): 1833-1839

Trager, W. and Jensen, J. B. (1976).Human malaria parasite in continuous culture. *Science* 193:673-675.

Woodrow, C. J., Haynes, R. K. and Krishna, S. (2005). Artemisinins. *Postgraduate Medical Journal.* 81(925): 71-78.

Zhang, S. & Gerhard, G. S. (2008). Heme activates artemisinin more efficiently than hemin, inorganic iron, or hemoglobin. *Bioorganic & Medicinal Chemistry.* 16(16): 7853-7861